

1 **Distinct genetic bases for plant root responses to lipo-chitooligosaccharide signal**
2 **molecules from distinct microbial origins**

3 Maxime Bonhomme^{1*}, Sandra Bensmihen^{2*,†}, Olivier André¹, Emilie Amblard¹, Magali
4 Garcia¹, Fabienne Maillet², Virginie Puech-Pagès¹, Clare Gough², Sébastien Fort³, Sylvain
5 Cottaz³, Guillaume Bécard¹, Christophe Jacquet^{1,†}

6

7 ¹ Laboratoire de Recherche en Sciences Végétales, Université de Toulouse, CNRS, UPS,
8 Castanet-Tolosan, France.

9 ² LIPM, Université de Toulouse, INRAE, CNRS, 31326 Castanet-Tolosan, France.

10 ³ Univ. Grenoble Alpes, CNRS, CERMAV, 38000 Grenoble, France.

11

12 * These authors contributed equally to this work

13 † authors for correspondence: Sandra.bensmihen@inrae.fr, phone +33 5 61 28 54 63
14 and jacquet@lrsv.ups-tlse.fr, phone : +33 (0)5 34 32 38 14

15

16

17 **ORCID**

18 **Maxime BONHOMME** : <https://orcid.org/0000-0002-1210-4777>

19 **Sandra BENSMIHEN** <https://orcid.org/0000-0003-1351-7220>

20 **Christophe JACQUET** : <https://orcid.org/0000-0002-7377-5638>

21

22

23

24

25

26

27

28

29

30

31 **Summary**

32

33 • Lipo-chitooligosaccharides (LCOs) were originally found as symbiotic signals called
34 Nod Factors (Nod-LCOs) controlling nodulation of legumes by rhizobia. More
35 recently LCOs were also found in symbiotic fungi and, more surprisingly, very widely
36 in the kingdom fungi including in saprophytic and pathogenic fungi. The LCO-
37 V(C18:1, Fuc/MeFuc), hereafter called Fung-LCOs, are the LCO structures most
38 commonly found in fungi. This raises the question of how legume plants, such as
39 *Medicago truncatula*, can perceive and discriminate between Nod-LCOs and these
40 Fung-LCOs.

41 • To address this question, we performed a Genome Wide Association Study on 173
42 natural accessions of *Medicago truncatula*, using a root branching phenotype and a
43 newly developed local score approach.

44 • Both Nod- and Fung-LCOs stimulated root branching in most accessions but there was
45 very little correlation in the ability to respond to these types of LCO molecules.
46 Moreover, heritability of root response was higher for Nod-LCOs than for Fung-
47 LCOs. We identified 123 loci for Nod-LCO and 71 for Fung-LCO responses, but only
48 one was common.

49 • This suggests that Nod- and Fung-LCOs both control root branching but use different
50 molecular mechanisms. The tighter genetic constraint of the root response to Fung-
51 LCOs possibly reflects the ancestral origin of the biological activity of these
52 molecules.

53

54

55

56 **Keywords:** GWAS, lateral root development, lipo-chitooligosaccharides, *Medicago*
57 *truncatula*, Nod Factors.

58

59

60

61

62

63

64 **Introduction**

65 Lipo-chitooligosaccharides (LCOs) belong to a family of chitin oligomers substituted on their
66 non-reducing end with an acyl chain, and further substituted with a variety of additional
67 functional groups. LCOs were originally found, 30 years ago, to be symbiotic signals, called
68 Nod factors, produced by rhizobia to trigger the nodulation process in legumes (Dénarié *et al.*,
69 1996). This discovery was the starting point for a series of work that gradually brought to
70 light the symbiotic signaling pathway required for rhizobial infection and nodulation in
71 legumes. The activation of this signaling pathway, now called the Common Symbiosis
72 Signalling Pathway (CSSP), was also found to be necessary for root colonization by
73 arbuscular mycorrhizal (AM) fungi (Catoira *et al.*, 2000). Furthermore, it was subsequently
74 discovered that LCOs with high structural similarity to Nod factors are also produced by AM
75 fungi (so called Myc-LCOs, Fig. S1) (Maillet *et al.*, 2011). Without genetic proof that these
76 molecules are essential for mycorrhization, but since they activate the CSSP as well as
77 symbiotic gene expression changes in host plants, they are considered, together with their
78 oligosaccharidic precursors (COs), as key mycorrhizal signals (Gough & Cullimore, 2011;
79 Genre *et al.*, 2013; Camps *et al.*, 2015; Sun *et al.*, 2015). This is supported by the recent
80 finding in *Solanum lycopersicum*, that the receptor protein SLYK10 binds Myc-LCOs and
81 controls the AM symbiosis (Girardin *et al.*, 2019). Also recently, Cope *et al.* showed both that
82 the CSSP is used for establishment of the ectomycorrhizal symbiosis between *Laccaria*
83 *bicolor* and poplar, and that *L. bicolor* can produce LCOs with similar structures to Nod
84 factors (Cope *et al.*, 2019). Possibly linked to their roles as symbiotic signals, LCOs can
85 interfere with immunity-related signaling in legumes (Rey *et al.*, 2019) and suppress innate
86 immune responses, even in the non-mycorrhizal plant *Arabidopsis thaliana* (Liang *et al.*,
87 2013). How LCOs dampen legume immunity is still unclear and controversial since they can
88 also induce defense gene expression (Nakagawa *et al.*, 2011). Another property of LCOs is
89 their ability to modify root architecture by stimulating Lateral Root Formation (LRF). The
90 stimulation of LRF appears to be a general response, observed in legume species such as
91 *Medicago truncatula* treated with Nod Factors or Myc-LCOs (Olah *et al.*, 2005; Maillet *et al.*,
92 2011), but also in the monocots rice and *Brachypodium distachyon* (Sun *et al.*, 2015; Buendia
93 *et al.*, 2019). Other positive effects of LCOs on soybean or maize root development are
94 reported (Souleimanov *et al.*, 2002; Tanaka *et al.*, 2015). So, up to this point in our

95 knowledge, LCOs were considered as signal molecules produced by a variety of symbiotic
96 microorganisms and with several effects on plants, including activation of the CSSP,
97 regulation of immune responses and stimulation of root development.

98 However, very recently, a new LCO chapter was opened when Rush *et al.* (Rush *et al.*, 2020)
99 discovered both that AM fungi produce a wider range of LCOs than previously described, and
100 that LCOs are not exclusive to symbiotic microorganisms, but are actually a family of
101 molecules commonly produced by a very large number of fungi, in all clades of the fungi
102 kingdom. As such, they will be thereafter referred to as “Fung-LCOs”. Like previously
103 characterized LCOs, Fung-LCOs consist of oligomers of 3- 5 residues of *N*-acetyl
104 glucosamine acylated with fatty acid chains of various length, saturated or not, and are
105 decorated with acetyl, *N* methyl, carbamoyl, fucosyl, fucosyl sulfate, methyl fucosyl or sulfate
106 groups. They can be found in phytopathogenic fungi, but also in saprophytes and
107 opportunistic human pathogens, *i.e.* in non-symbiotic fungi or in fungi that do not interact
108 with plants. The results of Rush *et al.* suggest that Fung-LCOs are conserved molecules in
109 fungi that can regulate endogenous developmental processes such as spore germination,
110 hyphal branching, or dimorphic switching. The fact that LCO-producing fungi of all kinds are
111 abundantly present in the close environment of plant roots raises many new questions.

112 Focusing on the plant side, some of these questions might be: are these Fung- LCO structures
113 able to trigger similar root responses, especially the LRF stimulation previously observed in
114 response to Nod- and Myc-LCOs? If so, are legumes nevertheless able to differentiate these
115 Fung-LCOs from the Nod-LCOs? To address these questions, we used a natural variability
116 approach to compare root growth responses to Fung-LCOs and Nod-LCOs, using the model
117 plant *Medicago truncatula*. As a legume, this plant must distinguish between Nod factors
118 specifically produced by its rhizobial symbiont, *Sinorhizobium meliloti*, and Fung-LCOs
119 molecules commonly produced by a vast number of rhizospheric fungi (Rush *et al.*, 2020).
120 We carried out two Genome-Wide Association Studies (GWAS) within a collection of 173
121 accessions of *M. truncatula* (Bonhomme *et al.*, 2014), whose seedlings have been either
122 treated with cognate Nod-LCOs, mainly LCO-IV(C16:2, Ac, S) or with the Fung-LCOs,
123 LCO-V(C18:1, Fuc/MeFuc) (Rush *et al.*, 2020). By doing so, we could compare root
124 responses to Nod- and Fung-LCOs in a way that is not possible using the reference A17
125 genotype and uncovered specific genetic determinants underlying these root responses. These
126 results shed light on how legumes can cope with rhizospheric structurally related signals
127 emitted by distinct microbes.

129 **Materials and Methods**

130 **Production of lipo-chitooligosaccharide molecules**

131 The Fung-LCOs used here were LCO-V(C18:1, Fuc/MeFuc) synthesized by
132 metabolically engineered *Escherichia coli* as described in (Samain *et al.*, 1997; Samain *et al.*,
133 1999; Ohsten Rasmussen *et al.*, 2004; Chambon *et al.*, 2015), the fucosyl and methylfucosyl
134 substitutions on the reducing end were obtained as described in (Djordjevic *et al.*, 2014). They
135 were chosen as they are the most representative of the fungal LCOs (Rush *et al.*, 2020).
136 *Sinorhizobium meliloti* Nod factors, named thereafter “Nod-LCOs” [mainly LCO-IV(C16:2,
137 Ac, S)] were extracted from *S. meliloti* culture supernatants by butanol extraction, and
138 purified by high-performance liquid chromatography (HPLC) on a semi-preparative C18
139 reverse phase column, as described in (Roche *et al.*, 1991b). Nod-LCO and Fung-LCO
140 structures (Fig. S1) were verified by mass spectrometry as described in (Cope *et al.*, 2019).

141

142 **Plant material, experimental design and root phenotyping**

143 A collection of 173 *M. truncatula* accessions (<http://www.medicagohapmap.org>) provided by
144 the INRAE *Medicago truncatula* Stock Center (Montpellier, France;
145 www1.montpellier.inra.fr/BRC-MTR/), was used for phenotyping experiments. These
146 accessions are representative of the overall genetic diversity of *M. truncatula* and belong to
147 the CC192 core collection (Ronfort *et al.*, 2006). GWAS for various phenotypic traits have
148 already been performed using this collection (Stanton-Geddes *et al.*, 2013; Bonhomme *et al.*,
149 2014; Yoder *et al.*, 2014; Kang *et al.*, 2015; Bonhomme *et al.*, 2019).

150 *M. truncatula* seeds were scarified with sulfuric acid, sterilized in bleach (2.5%) for four
151 minutes, washed in sterile water, and transferred on sterile agar plates for 2.5 days in the dark
152 at 15°C to synchronize germination. Seedlings were then grown *in vitro* on square Petri dishes
153 (12x12 cm) under 16 h light and 8 h dark at 22°C, with a 70° angle inclination, on modified
154 M-medium as described in (Bonhomme *et al.*, 2014). This medium contained either (i) the
155 “Nod” treatment in which Nod-LCOs were incorporated at a concentration of 10⁻⁸ M, (ii) the
156 “Fung” treatment in which Fung-LCOs, less water soluble than the sulfated Nod-LCOs, were
157 incorporated at a concentration of 10⁻⁷ M to ensure a final experimental concentration close to
158 10⁻⁸ M (Ohsten Rasmussen *et al.*, 2004), and (iii) two control (CTRL) conditions where
159 acetonitrile 50% was diluted 1000x (CTRL-Fung) and 10000x (CTRL-Nod). Each accession
160 of *M. truncatula* was phenotyped in two independent biological repeats, with 15 seedlings per

161 repeat (5 seedlings per plate), for each treatment (Nod, Fung, CTRL-Nod, CTRL-Fung).

162

163 For each treatment, the lateral root number (LR) of each seedling was followed at four
164 time points of plant development: 5, 8, 11 and 15 days after seedling transfer on LCO-
165 containing medium. In addition, the primary root length (RL) was measured 5- and 11-days
166 post treatment in order to calculate the lateral root density (LRD, *i.e.* the ratio of the lateral
167 root number over the primary root length of each plant). All these measurements were carried
168 out using the image analysis software Image J, using scans of plates. In order to summarize
169 the kinetics of lateral root number appearance over the four time points, we calculated for
170 each plant the Area Under the Lateral Root Progress Curve -AULRPC- (Fig. S2) using the R
171 statistical package “agricolae”. Overall, nine phenotypic variables were recorded for each
172 plant and for each treatment: LR_5d, LR_8d, LR_11d, LR_15d, RL_5d, RL_11d, LRD_5d,
173 LRD_11d and AULRPC.

174

175 **Statistical modeling of phenotypic data**

176 For the Nod and Fung treatments separately, as well as for the control of each
177 treatment (*i.e.* mock treated plants of the Nod- or Fung-LCOs experiments), adjusted means
178 of each accession (coefficients) were estimated for each of the nine phenotypic variables by
179 fitting the following linear model with fixed effects: $y_{ijk} = \text{accession}_i + \text{repeat}_j + \varepsilon_{ijk}$, where y_{ijk}
180 is the phenotypic value of the k th plant of the j th repeat for the i th accession. Since variation
181 in the root system development naturally occurred within and among accessions both in
182 control and Nod/Fung-treated plants, for LR, RL, LRD and AULRPC variables, an additional
183 variable of induction/repression of the root system development was estimated for each
184 accession by subtracting the coefficient value under treatment with Nod- or Fung-LCOs by
185 the coefficient value under control condition (*i.e.* CTRL-Nod or CTRL-Fung). GWAS was
186 performed using these variables, referred to as “delta”, estimated for each accession on Nod
187 and Fung-LCOs treatments separately (delta_LR_5d, delta_RL_5d, delta_LRD_5d,
188 delta_LR_8d, delta_LR_11d, delta_RL_11d, delta_LRD_11d, delta_LR_15d,
189 delta_AULRPC).

190

191 **Association mapping and local score analyses of phenotypic data**

192 GWAS was performed on the phenotypic variables described in the previous section,
193 based on phenotypic values for 173 accessions of *M. truncatula*. We used the Mt4.0
194 Medicago genome and SNP version to perform GWAS (see

195 <http://www.medicagohapmap.org/>). A set of 5,165,380 genome-wide SNPs was selected with
196 a minor allele frequency of 5% and at least 90% of the 173 accessions scored across the *M.*
197 *truncatula* collection. The statistical model used for GWAS was the mixed linear model
198 (MLM) approach implemented in the EMMA expedited (EMMAX) software (Kang *et al.*, 2010).
199 The MLM is used to estimate and then test for the significance of the allelic effect at each
200 SNP, taking into account the genetic relationships between individuals to reduce the false
201 positive rate. Genetic relationships among accessions were estimated using a kinship matrix
202 of pairwise genetic similarities which was based on the genome-wide proportion of alleles
203 shared between accessions, using the whole selected SNP dataset.

204 The MLM first implements a variance component procedure to estimate the genetic
205 (σ^2_a) and residual (σ^2_e) variances from the variance of the phenotypic data, by using the
206 kinship matrix in a restricted maximum likelihood framework. Narrow-sense heritabilities
207 (*i.e.* portion of the total phenotypic variation attributable to additive genetic effect, h^2_{ss}) of
208 each phenotypic variable were calculated from estimates of σ^2_a and σ^2_e . For each marker a
209 Generalized Least Square *F*-test is used to estimate the effects β_k and test the hypothesis $\beta_k =$
210 0 in the following model: $y_i = \beta_0 + \beta_k X_{ik} + \eta_i$, with X_{ik} the allele present in individual *i* for the
211 marker *k*, and η_i a combination of the random genetic and residual effects (Kang *et al.*, 2010).
212 As in previous GWAS in *M. truncatula* (Bonhomme *et al.*, 2014; Rey *et al.*, 2017), we used a
213 genome-wide 5% significance threshold with Bonferroni correction for the number of blocks
214 of SNPs in linkage disequilibrium (*i.e.* p -value $\leq 10^{-6}$), to identify significant associations
215 following the *F*-test on the estimated allele effect size at each SNP.

216 In order to detect small-effect QTL that would not pass the 10^{-6} significance threshold,
217 we performed a local score approach (Fariello *et al.*, 2017; Bonhomme *et al.*, 2019) on SNP
218 *p*-values. The local score is a cumulative score that takes advantage of local linkage
219 disequilibrium (LD) among SNPs. This score, defined as the maximum of the Lindley process
220 over a SNP sequence (*i.e.* a chromosome), as well as its significance threshold were
221 calculated based on EMAX *p*-values, using a tuning parameter value of $\xi = 3$, as suggested by
222 simulation results (Bonhomme *et al.*, 2019). R scripts used to compute the local score and
223 significance thresholds are available at <https://forge-dga.jouy.inra.fr/projects/local-score/documents>.

225

226 **Results**

227 **Natural variation in the stimulation of lateral root formation by Fung- and Nod-LCOs** 228 **in *M. truncatula***

229 The Fung-LCOs molecules used in this study belong to the class of LCOs most
230 commonly found in fungi (Rush *et al.*, 2020). They are LCO-V(C18:1,
231 Fucosylated/MeFucosylated). On the other hand, the Nod-LCOs are specific to the rhizobium
232 *S. meliloti* (Roche *et al.*, 1991b) that nodulates *M. truncatula*. These Nod-LCOs are mainly
233 LCO-IV(C16:2, Ac, S). The LCOs used therefore display some structural commonalities but
234 also some specificities (see Fig. S1).

235 Growth of the 173 accessions of *M. truncatula* in the presence of Fung-LCOs or Nod-
236 LCOs led to 67% and 87% of them with delta_AULRPC values above 0, respectively. This
237 suggests a global trend of LCO stimulation of lateral root formation (LRF), especially with
238 Nod-LCOs (Fig. 1a,b). This trend appeared early in the experiment since LRF was stimulated
239 in 72% and 83% of the accessions 5 days following Fung-LCO and Nod-LCO treatments,
240 respectively (Table 1). Among these accessions, the reference genotype A17 was strongly
241 stimulated by Nod-LCOs over the time course, but not by Fung-LCOs (Fig. 1a,b). Since LRF
242 stimulation showed substantial variation across the *M. truncatula* collection, we estimated the
243 heritability, namely the proportion of phenotypic variation observed that was due to genetic
244 variation in the collection (Table 1). In response to Fung-LCOs, the heritability was relatively
245 low ($h^2_{ss} \leq 0.16$) for phenotypic variables quantifying variation in lateral root (LR) number
246 and density, and showed a clear tendency to increase over time ($h^2_{ss} = 0.16$ for LR number at
247 15 days post treatment and $h^2_{ss} = 0.15$ for LR density at 11 days). In contrast, in response to
248 Nod-LCOs the heritability of variation in lateral root number and density was strong at early
249 times (i.e. 0.66 and 0.75 at 5 days post treatment, respectively) and decreased over time but
250 remained relatively high (i.e. > 0.22 and 0.35, respectively). Interestingly, variation of
251 primary root length in response to Fung- and Nod-LCOs was also observed. Its heritability
252 was stronger for Nod-LCOs at 11 days ($h^2_{ss} = 0.36$, Table 1). In the case of treatment with
253 Nod-LCOs, these results indicate that variation in LRF stimulation, but also in primary root
254 length stimulation, was largely due to genetic variation in the collection, especially at early
255 steps, showing the importance of natural variation in the genetic control of LRF and primary
256 root length stimulation by Nod-LCOs in *M. truncatula*. In the case of treatment with Fung-
257 LCOs, however, the strong level of LRF stimulation as well as the low heritability at early
258 steps ($0 \leq h^2_{ss} \leq 0.06$, see Table 1) support the hypothesis that the root response to Fung-
259 LCOs in *M. truncatula* is much more genetically constrained than the root response to Nod-
260 LCOs.

261 Since Fung and Nod-LCOs show a high structural homology and both stimulated LRF
262 in most genotypes, we tested whether accessions highly stimulated by Nod-LCOs were also

263 highly stimulated, not stimulated or even repressed by Fung-LCOs. Interestingly, for all
264 variables, we found no correlation between the stimulations by Fung- and Nod-LCOs, except
265 at 5 days where we found a significant but weak positive correlation for the variation in lateral
266 root number ($r = 0.15$, p -value = 0.024). The lack of global correlation between LRF
267 stimulation by Fung-LCOs and LRF stimulation by Nod-LCOs is illustrated in (Fig. 1c,d),
268 with the delta_AULRPC variable which captures root development over time, and with the
269 lateral root number at 5 days (delta_LR_5d) which captures early steps of root development.

270 Overall, these results suggest that (i) both Fung- and Nod-LCOs have the property to
271 stimulate LRF in a quantitative manner, and (ii) genetic variation seems more influential in
272 the root response to Nod-LCOs than to Fung-LCOs. To better understand the genetic
273 determinants underlying these contrasted phenotypic responses, we performed a Genome-
274 Wide Association Study.

275

276 **Genetic determinants underlying quantitative variation in root responsiveness to Fung- 277 and Nod-LCOs in *M. truncatula***

278 GWAS was performed separately for Fung and Nod-LCO treatments, for each of the
279 nine phenotypic variables measuring: (i) variation of the lateral root number (delta_LR_5d,
280 delta_LR_8d, delta_LR_11d and delta_LR_15d), (ii) lateral root density (delta_LRD_5d and
281 delta_LRD_11d), (iii) primary root length (delta_RL_5d, delta_RL_11d) and (iv) lateral root
282 progress curve (delta_AULRPC) over time (5, 8, 11 and 15 days). Across all phenotypic
283 variables measured in response to Fung-LCOs and Nod-LCOs, p -value-based tests performed
284 using EMMAx respectively identified 24 and 70 genomic regions or loci significant at the p -
285 value threshold of 10^{-6} . Using the local score approach, more significant candidate genomic
286 regions were identified as associated with root response to Fung- and Nod-LCOs, respectively
287 71 and 123 loci and 1 common locus (Table S1). All the loci identified with the EMMAx
288 approach are nested within the local score results. Identified loci contain 1 to 11 genes,
289 corresponding to 291 possible genes in total (see Table S1).

290 A global view of the genome-wide quantitative genetic bases of LRF stimulation
291 kinetics following treatment with LCOs could be obtained by the local score analysis of the
292 delta_AULRPC variable (Fig. 2a, b). Genetic variation involved in LRF stimulation
293 specifically in response to Fung-LCOs mainly relied on four candidate loci; a gibberellin 2-
294 oxidase (*Medtr1g086550*, GA2OX) and three receptor-like kinases: a putative Feronia
295 receptor-like kinase - *Medtr6g015805*-, a crinkly 4 receptor like kinase CCR4-like protein -
296 *Medtr3g464080* -, and a Serine/Threonine kinase PBS1 - *Medtr8g063300* - (Fig. 2a, Table

297 S1). One major locus on chromosome 7, containing genes from the leguminosin LEED.PEED
298 family (Trujillo *et al.*, 2014), but also kinase encoding genes with potential carbohydrate-
299 binding properties were specifically involved in response to Nod-LCOs (Fig. 2b, Table S1).
300 Only one candidate genomic region involved in the response to Fung-LCOs and Nod-LCOs
301 was identified in this study, by the GWAS analysis of delta_AULRPC and primary root
302 length (delta_RL_5d) phenotypic variables (Table S1). This region on chromosome 8 contains
303 three genes among which two encode “embryonic abundant protein”, annotated as BURP
304 domain-containing protein by the new *M. truncatula* genome version Mt5 (Pecrix *et al.*,
305 2018).

306 A more precise view of the genome-wide quantitative genetic bases of the early steps
307 of LRF stimulation following treatment with LCOs could be obtained by the local score
308 analysis of the delta_LRD_5d variable (Fig. 2c, d). Interestingly, this phenotypic variable
309 showed highly contrasted heritability values between treatments with Fung- and Nod-LCOs
310 ($h^2_{ss} = 0.06$ and 0.75, respectively; Table 1). Among 34 candidate genomic regions identified
311 in response to Fung-LCOs, we identified four highly significant candidate genes whose
312 predicted proteins show good homology for known functions, such as a dioxygenase
313 (*Medtr5g055800*), an LRR receptor-like kinase (*Medtr3g452970*), a WRKY family
314 transcription factor (*Medtr5g091390*) and a GRAS family transcription factor
315 (*Medtr4g097080*) whose homolog in *Arabidopsis thaliana* is SHORT-ROOT -SHR-
316 (Helariutta *et al.*, 2000). Among 49 candidate genomic regions identified in response to Nod-
317 LCOs for the delta_LRD_5d variable, we identified 4 highly significant candidate genes,
318 among which two encoded dioxygenases (*Medtr4g100590*, *Medtr2g068940*), one MYB
319 transcription factor (*Medtr5g081860*, MYB51) and the most significant one encoding a
320 putative membrane lipoprotein lipid attachment site-like protein (*Medtr8g464760*), annotated
321 as thioredoxin-like protein in Mt5 genome. This analysis also detected two known genes
322 encoding a sugar transporter (*Medtr3g098930*, MtSWEET11) and a GRAS family
323 transcription factor (*Medtr8g442410*, TF124) (Fig. 2d).

324

325 **Combination of GWAS results with Gene ontology classification highlights enrichment 326 in signaling functions**

327 GWAS most significant genes can give a first hint to determine some of the
328 mechanisms involved in root response to LCOs. However local score also highlighted minor
329 QTL/genes and allowed us to identify several dozen of supplementary genes. To gain further
330 insights from these data, we performed a Gene Ontology (GO) enrichment analysis using the

331 Medicago Superviewer interface (Herrbach *et al.*, 2017) (Fig. 3a,b). 71 and 134 genes
332 identified in the Fung-LCO and Nod-LCO GWAS were classified, respectively. At the
333 “biological process” level, both the Nod and Fung-LCO datasets were enriched in biological
334 functions related to “other metabolic processes”. The Nod-LCO data were also enriched in
335 transcription related biological processes. Although the Fung-LCO data did not show any
336 significant enrichment in transcription function at the “biological process” level, they were, as
337 the Nod-LCO data, enriched in transcription factor and kinase activities at the “molecular
338 function” level (Fig. 3 a,b). This is in accordance with the numerous loci associated with
339 Receptor-like kinases or transcription factors (TF) found in both datasets (see Table S1).
340 Accordingly, the Nod-LCO data showed enrichment in nuclear and plasma membrane
341 associated “cellular component” (Fig. 3b). Many of the metabolic functions from the Nod-
342 LCO candidates and of the genes underlying the “protein metabolism” biological process
343 enriched with Fung-LCOs were associated with phosphorylation, so possibly also with
344 signaling pathways. In addition, a significant proportion of loci were associated with oxido-
345 reduction processes and cell-wall metabolism enzymes (pectin-esterases, cellulose synthase,
346 phenylalanine ammonia-lyase-like protein). Although not specifically enriched in these
347 datasets, we also found several hormone related genes. For instance, auxin signaling
348 (AUX/IAA and Auxin Response Factor, ARF) and auxin transport (efflux carriers) genes
349 were found in the Nod-LCO data whereas an ethylene receptor and an ethylene responsive TF
350 were found in the Nod-LCO and Fung-LCO data, respectively (Table S1).
351 To gain further insight in possible biological processes where those loci could be involved, we
352 also compiled transcriptional expression data from the literature and the knowledge database
353 LEGOO (Carrère *et al.*, 2020). Data could be obtained for 148 out of the 291 candidate genes
354 and are summarized in Table S2. As expected, a majority of genes were found in symbiotic
355 studies (nodulation or mycorrhization, 123 genes) or with LCO treatments (25 genes among
356 which 23 are also found in the symbiotic data). However, available expression data was not
357 restricted to these symbiotic interactions. Indeed, expression data could also be retrieved from
358 nitrate or phosphate starvation experiments or from data obtained with *Medicago* root
359 pathogens or defense elicitors (Table S2).

360

361

362 **Discussion**

363 In this study, we asked whether a legume, here *M. truncatula*, is capable of
364 distinguishing lipo-chitooligosaccharide molecules that share similar structures and induce the
365 same developmental root responses. Regulation of root development by LCOs seems to be a
366 conserved plant response observed in legume and non-legume plants (Sun *et al.*, 2015;
367 Tanaka *et al.*, 2015; Buendia *et al.*, 2019), raising the question of its possible evolutionary
368 origin and molecular conservation. The Nod-LCO molecules we used, LCO-IV(C16:2, Ac,
369 S), are produced by the rhizobial symbiont of *M. truncatula*. These LCOs can be considered
370 as very specific symbiotic signals, with a key role in the narrow host specificity that
371 characterizes the rhizobium legume symbiosis (RLS). The simple absence of the sulfate group
372 on the reducing end of the Nod-LCOs renders them inactive symbiotically on *Medicago*
373 (Roche *et al.*, 1991a; Bensmihen *et al.*, 2011). In contrast, the Fung-LCO molecules used
374 here, LCO-V(C18:1, Fuc/MeFuc), are not only a form of LCOs commonly found in AM
375 fungi, but they can also be produced by pathogenic or saprophytic fungi (Rush *et al.*, 2020)
376 and can thus be considered as a common, almost universal, hallmark of fungal presence.
377 Furthermore, it is worth noticing that even *Bradyrhizobia* and *Sinorhizobium* symbionts of
378 soybean also produce LCO-V(C18:1, Fuc/MeFuc) (D'Haeze & Holsters, 2002; Wang *et al.*,
379 2018), making them also non cognate Nod-LCO signals. By studying the ability of *M.*
380 *truncatula* plants to respond to specific (Nod-LCOs) or wide-spread (Fung-LCOs) LCOs, we
381 were thus considering a common situation encountered by plants in their natural environment
382 where they must distinguish different LCO-producing microorganisms.

383 Here, we have exploited the large genetic diversity among *M. truncatula* natural
384 accessions using a GWAS approach to compare the genetic bases underlying root
385 developmental responses. The root phenotypic traits that we used, lateral root formation and
386 lateral root density, were chosen because in the *M. truncatula* A17 reference accession these
387 traits are stimulated by Nod factors and by the Myc-LCOs originally detected in AM fungi
388 (Fig. S1) (Olah *et al.*, 2005; Maillet *et al.*, 2011). To address LR density, we also looked at
389 primary root growth, a parameter that was not previously described as affected by Nod-LCOs
390 in A17. Moreover, these traits are relatively easy to score, which was convenient to phenotype
391 many accessions of *M. truncatula*.

392
393 **The Fung-LCO structures stimulate root development of *M. truncatula* in a quantitative**
394 **way**

395 Our results clearly show that the Fung-LCO molecules tested, LCO-V (C18:1,
396 Fuc/MeFuc) can also stimulate LRF in *M. truncatula*. This LRF stimulation is variable among
397 the accessions, and the trait would have been missed if we had only studied the reference
398 accession, A17, which is poorly responsive (Fig. 1), as previously shown with *Sinorhizobium*
399 *fredii* Nod factors, LCO-V (C18:1, MeFuc) (Olah *et al.*, 2005). Also, in contrast to what was
400 previously observed in A17 (Olah *et al.*, 2005), we could detect some positive effect of Nod-
401 LCOs on primary root length, especially at later time points (11 days). The majority of
402 accessions responded positively to Fung-LCOs for this growth parameter at both 5 and 11
403 days. Accordingly, we found a number of loci associated with the variation in primary root
404 length phenotype (Table S1). This underlines the power of the natural variation approach that
405 can detect more responsive genetic backgrounds and reveal new genetic determinants that
406 would have passed unnoticed in forward and reverse genetic screens with classical reference
407 accessions. Similarly, GWAS results obtained on root architecture modification of
408 *Arabidopsis thaliana* upon hormonal treatments identified that the Col-0 reference accession
409 is not the most responsive to auxin (Ristova *et al.*, 2018).

410

411 ***Medicago truncatula* can distinguish between Fung-LCOs and Nod-LCOs**

412 The lack of overlap, with only one exception and for different parameters, between the
413 loci identified in the Nod-LCO and Fung-LCO GWAS is striking. This lack of overlap is
414 consistent with the weak correlation between the ability of one accession to respond to Nod-
415 and to Fung-LCOs (Fig. 1). The absence of common genes (except one locus) highlighted in
416 the two GWAS, and the very different heritability values found associated with the Fung-
417 LCO and Nod-LCO responses, indicate that *M. truncatula* clearly distinguishes these signals,
418 although they have similar structures and cause the same root response. This can be due to
419 specific receptors (no data is available yet concerning plant receptors for the Fung-LCOs we
420 used) and/or to divergence in downstream signaling pathways. The latter hypothesis is
421 consistent with the enrichment in signaling functions we observed in the GWAS genes (Fig.
422 3). Nod-LCO and Myc-LCO stimulation of LRF requires the CSSP in *M. truncatula* (Olah *et*
423 *al.*, 2005; Maillet *et al.*, 2011). However, previous transcriptomic studies performed with
424 Myc-LCO structures which are closer to those of Nod-LCOs from *S. meliloti* (Fig. S1)
425 identified that Myc-LCO signaling can also act independently of the CSSP gene *MtDMI3*
426 (Czaja *et al.*, 2012; Camps *et al.*, 2015). It would be interesting to test whether the Fung-
427 LCOs we used here require signaling from the CSSP to activate the LRF responses in *M.*

428 *truncatula*. CSSP mutants are available in the *M. truncatula* A17 genetic background but this
429 accession is poorly responsive to these new Fung-LCOs in our assays (see Fig. 1).

430

431 **Genetic determinants of *M. truncatula* responses to Fung-LCOs and Nod-LCOs**

432 *Cell wall, root growth and developmental signaling pathways associated loci*

433 Only one of the genes or loci identified in the two GWAS analyses was found to be
434 common. This region contained two genes annotated as BURP domain-containing proteins,
435 which define a group of proteins specific to plants (Table S1). This domain was named from
436 the four members of the group initially identified, BNM2, USP, RD22, and PG1beta and is
437 commonly found in plant cell wall proteins (Hattori *et al.*, 1998; Wang *et al.*, 2015). Cell-wall
438 related functions, like-cell-wall remodeling, could be linked to root growth promotion
439 activities of the LCO molecules, and additionally might be related to the root hair deformation
440 capacities of LCOs (Esseling *et al.*, 2003). One gene associated with this locus
441 (*Medtr8g046000*) was previously described as down-regulated by Nod-LCOs in the root
442 epidermis (4h after 10^{-8} M Nod-LCO treatment) (Jardinaud *et al.*, 2016), downregulated in
443 nodules at 4 and 10 dpi, compared to roots (El Yahyaoui *et al.*, 2004) and upregulated in roots
444 mycorrhized with *Rhizophagus irregularis* at 28 dpi compared to non-mycorrhizal control
445 roots (Hogekamp *et al.*, 2011) (see Table S2).

446 In the Fung-LCO GWAS, we found some signaling genes that could have a role in
447 LRF. These are the receptor like kinase (RLK) CRINKLY 4 (CCR4) (*Medtr3g464080*), and a
448 GRAS TF (*Medtr4g097080*) related to the *SHORTROOT* gene of *Arabidopsis*, known to
449 control root development (Helariutta *et al.*, 2000; De Smet *et al.*, 2008), although neither of
450 these two genes has been characterized in *M. truncatula*. Among the putative RLK genes
451 detected in the Fung-LCO GWAS, there was also one that could encode a Feronia RLK
452 (*Medtr6g015805*). Interestingly, this protein regulates root growth of *A. thaliana* (Haruta *et*
453 *al.*, 2014) but also plant immune signaling by sensing cell-wall integrity (Stegmann *et al.*,
454 2017), two biological processes also regulated by LCOs. Similarly, we identified several
455 receptor-like cytosolic kinases (RLCKs), also known as PBS1-like kinases, from the
456 subfamily VII in the Nod-LCO data. Some genes from this subfamily are involved in PAMP-
457 triggered immunity (PTI), including chitin responses in *A. thaliana* (Rao *et al.*, 2018).

458 *Phytohormone associated loci*

459 Relatively few hormone-related genes were identified in the two GWAS and they were
460 all different. The ethylene-related genes *Medtr1g069985* and *Medtr1g073840* were found in

461 Fung-LCO and Nod-LCO GWAS, respectively. A gibberellin-related GA2 oxidase gene
462 (*Medtr1g086550*) and a few auxin transporter genes (*Medtr5g024530*, *Medtr5g024560* and
463 *Medtr5g024580*) were found in the Fung-LCO and Nod-LCO GWAS, respectively. GA2
464 oxidase is predicted to be a catabolic enzyme that degrades gibberellins (GA) (Yamaguchi,
465 2008). In *M. truncatula*, in contrast to Arabidopsis, GAs are negative regulators of LRF
466 (Fonouni-Farde *et al.*, 2019). They are also negative regulators of nodulation and
467 mycorrhization (Foo *et al.*, 2013; Bensmihen, 2015) so down regulation of the GA content
468 could stimulate LRF, nodulation and mycorrhization. Interestingly, all the auxin-related
469 functions were found in the Nod-LCO GWAS only. This could be related to the tight
470 developmental links between LR formation and nodule organogenesis and their common need
471 for auxin accumulation in *M. truncatula* (Schiessl *et al.*, 2019; Soyano *et al.*, 2019).

472 *Endosymbiosis associated loci*

473 Several other loci we identified could also be related to symbiosis. When comparing
474 with previous transcriptomic studies, we found 123 genes (78 for Nod-LCOs, 44 for Fung-
475 LCOs and one found in both studies) expressed during symbiotic processes (nodulation or
476 mycorrhization, Table S2). This represents an important overlap probably linked to the role of
477 these molecules as pre-symbiotic or symbiotic signals to prepare for specific symbiotic
478 events. We could even find some very specific LEED...PEED loci that are only expressed in
479 nodules (Trujillo *et al.*, 2014). Along the same line, *MtSWEET11* (found for the difference in
480 LRD at 5 days with Nod-LCOs, Table S1) was previously shown to be expressed in infected
481 root hairs, and more specifically in infection threads and symbiosomes during nodulation in
482 *M. truncatula*. However, knock out of this gene did not impair RLS, possibly due to genetic
483 redundancy (Kryvoruchko *et al.*, 2016). This illustrates the interest of GWAS to identify
484 genes without any redundancy issues. Some genes identified in our Nod-LCO GWAS were
485 also found in a previous GWAS of nodulation. For example,
486 *Medtr1g064090/Medtr1te064120* (annotated as a phenylalanine ammonia-lyase-like protein /
487 Copia-like polyprotein/retrotransposon) and *Medtr2g019990* (annotated as a
488 Serine/Threonine-kinase PBS1-like protein) were previously found by Stanton-Geddes and
489 colleagues as associated with nodule numbers in the lower part of the root (Stanton-Geddes *et*
490 *al.*, 2013). Two other loci *Medtr3g034160* (galactose oxidase) and *Medtr5g085100* (AP2
491 domain class transcription factor) were respectively found as associated with nodule numbers
492 in the upper part of the root and with strain occupancy in the lower part of the root (Stanton-
493 Geddes *et al.*, 2013).

494 We did not find any known CSSP or LysM-RLK genes among our loci detected by GWAS.
495 This is somehow expected as constrained natural variability on these essential symbiotic
496 genes due to selective processes was often found in previous nucleotide polymorphism
497 analyses (De Mita *et al.*, 2006; De Mita *et al.*, 2007; Grillo *et al.*, 2016) and in previous
498 GWAS studies performed on nodulation phenotypes (Stanton-Geddes *et al.*, 2013). This also
499 suggests that these genes are not major determinants of natural variability in root
500 developmental responses to LCOs, although some LysM-RLK genetic variants likely account
501 for rhizobia host-specificity (Sulima *et al.*, 2017; Sulima *et al.*, 2019).

502

503 **Evolutionary origin of *M. truncatula* responses to Fung-LCOs and Nod-LCOs**

504 Our GWAS results also raise interesting questions on the evolutionary origin of the
505 root growth stimulation role of LCOs. Indeed, the two different LCO structures (from
506 different microbial origins) triggered LRF stimulation on a high number of *Medicago*
507 accessions. The low heritability of plant responses to Fung-LCOs (with a maximum of 0.16
508 for the difference in LR number at 15 days), compared to that of plant responses to Nod-
509 LCOs (with a maximum of 0.75 for lateral root density at 5 days) is not due to a lack of
510 activity of the Fung-LCOs since 67% to 76% of the accessions did show a positive root
511 growth response to these LCOs. This rather suggests that the genetic determinants of the
512 Fung-LCO responses are more “fixed” (*i.e.* less variable) than those of the Nod-LCO
513 responses. The low genetic variability of responses to these widespread Fung-LCO structures
514 is likely linked to their very ancient apparition in the fungi kingdom (Rush *et al.*, 2020), and
515 suggests that the ancient function(s) of these LCOs were non symbiotic. Ancient LCO
516 functions could be LRF stimulation or the regulation of immunity in plants (Liang *et al.*,
517 2013; Limpens *et al.*, 2015; Feng *et al.*, 2019), a function that may have predated the
518 mycorrhizal symbiosis and has not been lost in *Arabidopsis* (Liang *et al.*, 2014). LCOs could
519 also be involved in other aspects of plant biology, yet to be discovered.

520

521 **Conclusion**

522 In addition to providing many new genes potentially involved in regulating root
523 development for future reverse genetic or allelic variant investigations, this study brings new
524 evidence that plants can distinguish between specific and non-specific LCO signals and
525 suggests that their recognition has had distinct evolutionary histories.

526

527 **Acknowledgments**

528 This work was part of a program funded by the French Agence Nationale de la Recherche
529 (ANR-14-CE18-0008, "NICE CROPS"). The authors thank the bioinformatics platform
530 Toulouse Midi-Pyrénées (Genotoul). Thanks to V. Regard for help with formatting of
531 TableS2. Mass spectrometry analyses were done with the support from the ICT-Mass
532 Spectrometry and MetaToul-AgromiX facilities and from the MetaboHUB-ANR-11-INBS-
533 0010 network. S.F. and S.C. received technical support of ICMG (FR 2607) mass
534 spectrometry platform and partial financial support from the LABEX ARCANE and CBH-
535 EUR-GS (ANR-17-EURE-0003), Glyco@Alps (ANR-15-IDEX-02), and PolyNat Carnot
536 Institut (ANR-16-CARN-0025-01). This work was performed in the LRSV and LIPM
537 (Toulouse, France), parts of the "Laboratoire d'Excellence" (LABEX) entitled TULIP (ANR-
538 10-LABX-41).

539

540

541 **Author contributions**

542 MB, SB: analyzed the data; MB, SB, CG, GB, CJ: wrote the manuscript; MB, GB, CG, CJ:
543 designed the experiments; OA, EA, MG, FM, VPP: performed the experiments; SF, SC:
544 synthesized the Fung-LCO molecules.

545

546 **References**

547 **Bensmihen S. 2015.** Hormonal Control of Lateral Root and Nodule Development in
548 Legumes. *Plants (Basel)* **4**(3): 523-547.

549 **Bensmihen S, de Billy F, Gough C. 2011.** Contribution of NFP LysM Domains to the
550 Recognition of Nod Factors during the *Medicago truncatula*/*Sinorhizobium meliloti*
551 Symbiosis. *PLoS One* **6**(11): e26114.

552 **Bonhomme M, André O, Badis Y, Ronfort J, Burgarella C, Chantret N, Prosperi JM,
553 Briskine R, Mudge J, Debéillé F, et al. 2014.** High-density genome-wide association
554 mapping implicates an F-box encoding gene in *Medicago truncatula* resistance to
555 *Aphanomyces euteiches*. *New Phytol* **201**(4): 1328-1342.

556 **Bonhomme M, Fariello MI, Navier H, Hajri A, Badis Y, Miteul H, Samac DA, Dumas B,
557 Baranger A, Jacquet C, et al. 2019.** A local score approach improves GWAS
558 resolution and detects minor QTL: application to *Medicago truncatula* quantitative

559 disease resistance to multiple *Aphanomyces euteiches* isolates. *Heredity (Edinb)*
560 **123**(4): 517-531.

561 **Buendia L, Maillet F, O'Connor D, van de-Kerkhove Q, Danoun S, Gough C, Lefebvre**
562 **Bensmihen S. 2019.** Lipo-chitooligosaccharides promote lateral root formation and
563 modify auxin homeostasis in *Brachypodium distachyon*. *New Phytol* **221**(4): 2190-
564 2202.

565 **Camps C, Jardinaud MF, Rengel D, Carrère S, Hervé C, Debelle F, Gamas P,**
566 **Bensmihen S, Gough C. 2015.** Combined genetic and transcriptomic analysis reveals
567 three major signalling pathways activated by Myc-LCOs in *Medicago truncatula*. *New*
568 *Phytol* **208**(1): 224-240.

569 **Carrère SB, Verdenaud M, Gough C, Gouzy JRM, Gamas P. 2020.** LeGOO: An
570 Expertized Knowledge Database for the Model Legume *Medicago truncatula*. *Plant*
571 *Cell Physiol* **61**(1): 203-211.

572 **Catoira R, Galera C, de Billy F, Penmetsa RV, Journet EP, Maillet F, Rosenberg C,**
573 **Cook D, Gough C, Dénarié J. 2000.** Four genes of *Medicago truncatula* controlling
574 components of a nod factor transduction pathway. *Plant Cell* **12**(9): 1647-1666.

575 **Chambon R, Desprás G, Brossay A, Vauzeilles B, Urban D, Beau JM, Armand S, Cottaz**
576 **S, Fort S. 2015.** Efficient chemoenzymatic synthesis of lipo-chitin oligosaccharides as
577 plant growth promoters. *Green Chem.* **17**: 3923-3930.

578 **Cope KR, Bascaules A, Irving TB, Venkateshwaran M, Maeda J, Garcia K, Rush TA,**
579 **Ma C, Labbé J, Jawdy S, et al. 2019.** The Ectomycorrhizal Fungus *Laccaria bicolor*
580 Produces Lipochitooligosaccharides and Uses the Common Symbiosis Pathway to
581 Colonize *Populus* Roots. *Plant Cell* **31**(10): 2386-2410.

582 **Czaja LF, Hogeboom C, Lamm P, Maillet F, Martinez EA, Samain E, Dénarié J, Küster**
583 **H, Hohnjec N. 2012.** Transcriptional responses toward diffusible signals from
584 symbiotic microbes reveal MtNFP- and MtDMI3-dependent reprogramming of host
585 gene expression by arbuscular mycorrhizal fungal lipochitooligosaccharides. *Plant*
586 *Physiol* **159**(4): 1671-1685.

587 **D'Haeze W, Holsters M. 2002.** Nod factor structures, responses, and perception during
588 initiation of nodule development. *Glycobiology* **12**(6): 79R-105R.

589 **De Mita S, Santoni S, Hochu I, Ronfort J, Bataillon T. 2006.** Molecular evolution and
590 positive selection of the symbiotic gene NORK in *Medicago truncatula*. *J Mol Evol*
591 **62**(2): 234-244.

592 **De Mita S, Santoni S, Ronfort J, Bataillon T. 2007.** Adaptive evolution of the symbiotic
593 gene NORK is not correlated with shifts of rhizobial specificity in the genus
594 *Medicago*. *Bmc Evolutionary Biology* **7**:210.

595 **De Smet I, Vassileva V, De Rybel B, Levesque MP, Grunewald W, Van Damme D, Van**
596 **Noorden G, Naudts M, Van Isterdael G, De Clercq R, et al. 2008.** Receptor-like
597 kinase ACR4 restricts formative cell divisions in the *Arabidopsis* root. *Science*
598 **322**(5901): 594-597.

599 **Djordjevic MA, Bezios A, Susanti, Marmuse L, Driguez H, Samain E, Vauzeilles B, Beau**
600 **JM, Kordbacheh F, Rolfe BG, et al. 2014.** Lipo-chitin oligosaccharides, plant
601 symbiosis signalling molecules that modulate mammalian angiogenesis in vitro. *PLoS*
602 **One** **9**(12): e112635.

603 **Dénarié J, Debelle F, Promé JC. 1996.** Rhizobium lipo-chitooligosaccharide nodulation
604 factors: signaling molecules mediating recognition and morphogenesis. *Annu Rev*
605 *Biochem* **65**: 503-535.

606 **El Yahyaoui F, Kuster H, Ben Amor B, Hohnjec N, Puhler A, Becker A, Gouzy J,**
607 **Vernie T, Gough C, Niebel A, et al. 2004.** Expression profiling in *Medicago*
608 *truncatula* identifies more than 750 genes differentially expressed during nodulation,
609 including many potential regulators of the symbiotic program. *Plant Physiol* **136**(2):
610 3159-3176.

611 **Esseling JJ, Lhuissier FG, Emons AM. 2003.** Nod factor-induced root hair curling:
612 continuous polar growth towards the point of nod factor application. *Plant Physiol*
613 **132**(4): 1982-1988.

614 **Fariello MI, Boitard S, Mercier S, Robelin D, Faraut T, Arnould C, Recoquillay J,**
615 **Bouchez O, Salin G, Dehais P, et al. 2017.** Accounting for linkage disequilibrium in
616 genome scans for selection without individual genotypes: The local score approach.
617 *Mol Ecol* **26**(14): 3700-3714.

618 **Feng F, Sun J, Radhakrishnan GV, Lee T, Bozsóki Z, Fort S, Gavrin A, Gysel K,**
619 **Thygesen MB, Andersen KR, et al. 2019.** A combination of chitooligosaccharide
620 and lipochitooligosaccharide recognition promotes arbuscular mycorrhizal
621 associations in *Medicago truncatula*. *Nat Commun* **10**(1): 5047.

622 **Fonouni-Farde C, Miassod A, Laffont C, Morin H, Bendahmane A, Diet A, Frugier F.**
623 **2019.** Gibberellins negatively regulate the development of *Medicago truncatula* root
624 system. *Sci Rep* **9**(1): 2335.

625 **Foo E, Ross JJ, Jones WT, Reid JB. 2013.** Plant hormones in arbuscular mycorrhizal
626 symbioses: an emerging role for gibberellins. *Ann Bot* **111**(5): 769-779.

627 **Genre A, Chabaud M, Balzergue C, Puech-Pagès V, Novero M, Rey T, Fournier J,**
628 **Rochange S, Bécard G, Bonfante P, et al. 2013.** Short-chain chitin oligomers from
629 arbuscular mycorrhizal fungi trigger nuclear Ca²⁺ spiking in *Medicago truncatula*
630 roots and their production is enhanced by strigolactone. *New Phytol* **198**(1): 190-202.

631 **Girardin A, Wang T, Ding Y, Keller J, Buendia L, Gaston M, Ribeyre C, Gascioli V,**
632 **Auriac M-C, Vernie T, et al. 2019.** LCO Receptors Involved in Arbuscular
633 Mycorrhiza Are Functional for Rhizobia Perception in Legumes. *Current Biology*
634 **29**(24):4249-4259.e5.

635 **Gough C, Cullimore J. 2011.** Lipo-chitooligosaccharide signaling in endosymbiotic plant-
636 microbe interactions. *Mol Plant Microbe Interact* **24**(8): 867-878.

637 **Grillo MA, De Mita S, Burke PV, Solórzano-Lowell KL, Heath KD. 2016.** Intrapopulation
638 genomics in a model mutualist: Population structure and candidate symbiosis genes
639 under selection in *Medicago truncatula*. *Evolution* **70**(12): 2704-2717.

640 **Haruta M, Sabat G, Stecker K, Minkoff BB, Sussman MR. 2014.** A peptide hormone and
641 its receptor protein kinase regulate plant cell expansion. *Science* **343**(6169): 408-411.

642 **Hattori J, Boutilier KA, van Lookeren Campagne MM, Miki BL. 1998.** A conserved
643 BURP domain defines a novel group of plant proteins with unusual primary structures.
644 *Mol Gen Genet* **259**(4): 424-428.

645 **Helariutta Y, Fukaki H, Wysocka-Diller J, Nakajima K, Jung J, Sena G, Hauser MT,**
646 **Benfey PN. 2000.** The SHORT-ROOT gene controls radial patterning of the
647 *Arabidopsis* root through radial signaling. *Cell* **101**(5): 555-567.

648 **Herrbach V, Chirinos X, Rengel D, Agbevenou K, Vincent R, Pateyron S, Huguet S,**
649 **Balzergue S, Pasha A, Provart N, et al. 2017.** Nod factors potentiate auxin signaling
650 for transcriptional regulation and lateral root formation in *Medicago truncatula*. *J Exp*
651 *Bot* **68**(3): 569-583.

652 **Hogekamp C, Arndt D, Pereira PA, Becker JD, Hohnjec N, Küster H. 2011.** Laser
653 microdissection unravels cell-type-specific transcription in arbuscular mycorrhizal
654 roots, including CAAT-box transcription factor gene expression correlating with
655 fungal contact and spread. *Plant Physiol* **157**(4): 2023-2043.

656 **Jardinaud MF, Boivin S, Rodde N, Catrice O, Kisiala A, Lepage A, Moreau S, Roux B,**
657 **Cottret L, Sallet E, et al. 2016.** A laser dissection-RNAseq analysis highlights the

658 activation of cytokinin pathways by Nod factors in the *Medicago truncatula* root
659 epidermis. *Plant Physiol.* 171(3):2256-76.

660 **Kang HM, Sul JH, Service SK, Zaitlen NA, Kong SY, Freimer NB, Sabatti C, Eskin E.**
661 **2010.** Variance component model to account for sample structure in genome-wide
662 association studies. *Nat Genet* 42(4): 348-354.

663 **Kang Y, Sakiroglu M, Krom N, Stanton-Geddes J, Wang M, Lee YC, Young ND,**
664 **Udvardi M. 2015.** Genome-wide association of drought-related and biomass traits
665 with HapMap SNPs in *Medicago truncatula*. *Plant Cell Environ.* 38(10):1997-2011.

666 **Kryvoruchko IS, Sinharoy S, Torres-Jerez I, Sosso D, Pislariu CI, Guan D, Murray J,**
667 **Benedito VA, Frommer WB, Udvardi MK. 2016.** MtSWEET11, a Nodule-Specific
668 Sucrose Transporter of *Medicago truncatula*. *Plant Physiol* 171(1): 554-565.

669 **Liang Y, Cao Y, Tanaka K, Thibivilliers S, Wan J, Choi J, Kang C, Qiu J, Stacey G.**
670 **2013.** Nonlegumes respond to rhizobial Nod factors by suppressing the innate immune
671 response. *Science* 341(6152): 1384-1387.

672 **Liang Y, Tóth K, Cao Y, Tanaka K, Espinoza C, Stacey G. 2014.**
673 Lipochitooligosaccharide recognition: an ancient story. *New Phytol* 204(2): 289-296.

674 **Limpens E, van Zeijl A, Geurts R. 2015.** Lipochitooligosaccharides modulate plant host
675 immunity to enable endosymbioses. *Annu Rev Phytopathol* 53: 311-334.

676 **Maillet F, Poinsot V, André O, Puech-Pages V, Haouy A, Gueunier M, Cromer L,**
677 **Giraudet D, Formey D, Niebel A, et al. 2011.** Fungal lipochitooligosaccharide
678 symbiotic signals in arbuscular mycorrhiza. *Nature* 469(7328): 58-63.

679 **Nakagawa T, Kaku H, Shimoda Y, Sugiyama A, Shimamura M, Takanashi K, Yazaki**
680 **K, Aoki T, Shibuya N, Kouchi H. 2011.** From defense to symbiosis: limited
681 alterations in the kinase domain of LysM receptor-like kinases are crucial for
682 evolution of legume-Rhizobium symbiosis. *Plant J.* 65(2):169-80.

683 **Ohsten Rasmussen M, Hogg B, Bono JJ, Samain E, Driguez H. 2004.** New access to lipo-
684 chitooligosaccharide nodulation factors. *Org Biomol Chem* 2(13): 1908-1910.

685 **Olah B, Briere C, Bécard G, Dénarié J, Gough C. 2005.** Nod factors and a diffusible factor
686 from arbuscular mycorrhizal fungi stimulate lateral root formation in *Medicago*
687 *truncatula* via the DMI1/DMI2 signalling pathway. *Plant J* 44(2): 195-207.

688 **Pecrix Y, Staton SE, Sallet E, Lelandais-Brere C, Moreau S, Carrere S, Blein T,**
689 **Jardinaud MF, Latrasse D, Zouine M, et al. 2018.** Whole-genome landscape of
690 *Medicago truncatula* symbiotic genes. *Nature Plants* 4(12): 1017-1025.

691 **Rao S, Zhou Z, Miao P, Bi G, Hu M, Wu Y, Feng F, Zhang X, Zhou JM. 2018.** Roles of
692 Receptor-Like Cytoplasmic Kinase VII Members in Pattern-Triggered Immune
693 Signaling. *Plant Physiol* **177**(4): 1679-1690.

694 **Rey T, Andre O, Nars A, Dumas B, Gough C, Bottin A, Jacquet C. 2019.** Lipo-
695 chitooligosaccharide signalling blocks a rapid pathogen-induced ROS burst without
696 impeding immunity. *New Phytologist* **221**(2): 743-749.

697 **Rey T, Bonhomme M, Chatterjee A, Gavrin A, Toulotte J, Yang W, André O, Jacquet
698 C, Schornack S. 2017.** The *Medicago truncatula* GRAS protein RAD1 supports
699 arbuscular mycorrhiza symbiosis and Phytophthora palmivora susceptibility. *J Exp
700 Bot* **68**(21-22): 5871-5881.

701 **Ristova D, Giovannetti M, Metesch K, Busch W. 2018.** Natural genetic variation shapes
702 root system responses to phytohormones in *Arabidopsis*. *Plant J* **96**(2): 468-481.

703 **Roche P, Debelle F, Maillet F, Lerouge P, Faucher C, Truchet G, Dénarié J, Promé JC.
704 1991a.** Molecular basis of symbiotic host specificity in *Rhizobium meliloti*: nodH and
705 nodPQ genes encode the sulfation of lipo-oligosaccharide signals. *Cell* **67**(6): 1131-
706 1143.

707 **Roche P, Lerouge P, Ponthus C, Prome JC. 1991b.** Structural determination of bacterial
708 nodulation factors involved in the *Rhizobium meliloti*-alfalfa symbiosis. *J Biol Chem*
709 **266**(17): 10933-10940.

710 **Ronfort J, Bataillon T, Santoni S, Delalande M, David JL, Prosperi JM. 2006.**
711 Microsatellite diversity and broad scale geographic structure in a model legume:
712 building a set of nested core collection for studying naturally occurring variation in
713 *Medicago truncatula*. *BMC Plant Biol* **6**: 28.

714 **Rush T, Puech-Pagès V, Bascaules A, Jargeat P, Maillet F, Haouy A, Maës A, Carrera
715 Carriel C, Khokhani D, Keller-Pearson M, et al. 2020.** Lipo-chitooligosaccharides
716 as regulatory signals of fungal growth and development. *Nature Commun* **in press**.

717 **Samain E, Chazalet V, Geremia RA. 1999.** Production of O-acetylated and sulfated
718 chitooligosaccharides by recombinant *Escherichia coli* strains harboring different
719 combinations of nod genes. *J Biotechnol* **72**(1-2): 33-47.

720 **Samain E, Drouillard S, Heyraud A, Driguez H, Geremia RA. 1997.** Gram-scale synthesis
721 of recombinant chitooligosaccharides in *Escherichia coli*. *Carbohydr Res* **302**(1-2):
722 35-42.

723 **Schiessl K, Lilley JLS, Lee T, Tamvakis I, Kohlen W, Bailey PC, Thomas A, Luptak J,
724 Ramakrishnan K, Carpenter MD, et al. 2019.** NODULE INCEPTION Recruits the

725 Lateral Root Developmental Program for Symbiotic Nodule Organogenesis in
726 *Medicago truncatula*. *Curr Biol.* 29(21):3657-3668.e5

727 **Souleimanov A, Prithiviraj B, Smith DL. 2002.** The major Nod factor of *Bradyrhizobium*
728 *japonicum* promotes early growth of soybean and corn. *J Exp Bot* 53(376): 1929-1934.

729 **Soyano T, Shimoda Y, Kawaguchi M, Hayashi M. 2019.** A shared gene drives lateral root
730 development and root nodule symbiosis pathways in Lotus. *Science* 366(6468): 1021-
731 1023.

732 **Stanton-Geddes J, Paape T, Epstein B, Briskine R, Yoder J, Mudge J, Bharti AK,**
733 **Farmer AD, Zhou P, Denny R, et al. 2013.** Candidate genes and genetic architecture
734 of symbiotic and agronomic traits revealed by whole-genome, sequence-based
735 association genetics in *Medicago truncatula*. *PLoS One* 8(5): e65688.

736 **Stegmann M, Monaghan J, Smakowska-Luzan E, Rovenich H, Lehner A, Holton N,**
737 **Belkhadir Y, Zipfel C. 2017.** The receptor kinase FER is a RALF-regulated scaffold
738 controlling plant immune signaling. *Science* 355(6322): 287-289.

739 **Sulima AS, Zhukov VA, Afonin AA, Zhernakov AI, Tikhonovich IA, Lutova LA. 2017.**
740 Selection Signatures in the First Exon of Paralogous Receptor Kinase Genes from the
741 Sym2 Region of the *Pisum sativum* L. Genome. *Frontiers in Plant Science* 8:1957

742 **Sulima AS, Zhukov VA, Kulaeva OA, Vasileva EN, Borisov AY, Tikhonovich IA. 2019.**
743 New sources of *Sym2^A* allele in the pea (*Pisum sativum* L.) carry the unique variant
744 of candidate LysM-RLK gene *LykX*. *PeerJ* 7: e8070.

745 **Sun J, Miller JB, Granqvist E, Wiley-Kalil A, Gobbato E, Maillet F, Cottaz S, Samain E,**
746 **Venkateshwaran M, Fort S, et al. 2015.** Activation of symbiosis signaling by
747 arbuscular mycorrhizal fungi in legumes and rice. *Plant Cell* 27(3): 823-838.

748 **Tanaka K, Cho SH, Lee H, Pham AQ, Batek JM, Cui S, Qiu J, Khan SM, Joshi T,**
749 **Zhang ZJ, et al. 2015.** Effect of lipo-chitooligosaccharide on early growth of C4
750 grass seedlings. *J Exp Bot* 66(19): 5727-5738.

751 **Trujillo DI, Silverstein KA, Young ND. 2014.** Genomic characterization of the
752 LEED..PEEDs, a gene family unique to the medicago lineage. *G3 (Bethesda)* 4(10):
753 2003-2012.

754 **Wang D, Couderc F, Tian CF, Gu W, Liu LX, Poinsot V. 2018.** Conserved Composition of
755 Nod Factors and Exopolysaccharides Produced by Different Phylogenetic Lineage.
756 *Front Microbiol* 9: 2852.

757 **Wang L, Wu N, Zhu Y, Song W, Zhao X, Li Y, Hu Y. 2015.** The divergence and positive
758 selection of the plant-specific BURP-containing protein family. *Ecol Evol* **5**(22):
759 5394-5412.

760 **Yamaguchi S. 2008.** Gibberellin metabolism and its regulation. *Annu Rev Plant Biol* **59**: 225-
761 251.

762 **Yoder JB, Stanton-Geddes J, Zhou P, Briskine R, Young ND, Tiffin P. 2014.** Genomic
763 signature of adaptation to climate in *Medicago truncatula*. *Genetics* **196**(4): 1263-
764 1275.

765

766

767

768

769

770

771 **Supplemental Figures**

772 **Figure S1. Structures of the LCOs used in this study compared to the “original” Myc-
773 LCOs described in Maillet *et al.*, 2011.**

774

775 **Figure S2. Lateral root formation phenotypic variables used in this study.**

776

777

778

779

780

781

782

783

784

785

786

787

788

789

790

791

792

793

794

795 **Tables**

796 **Table 1 – Estimation of narrow-sense heritability for different phenotypic variables**
797 **measuring lateral root stimulation.**

Days post treatment	Fung-LCO treatment		Nod-LCO treatment		
	Heritability	% accessions with $\Delta > 0$ (stimulation)	Heritability	% accessions with $\Delta > 0$ (stimulation)	
$\Delta_{\text{lateral_root_number}}$	5	0	71.7 (++)	0.66	82.7 (++)
$\Delta_{\text{lateral_root_number}}$	8	0.03	75.7 (++)	0.48	90.2 (+++)
$\Delta_{\text{lateral_root_number}}$	11	0.11	75.1 (++)	0.22	82.1 (++)
$\Delta_{\text{lateral_root_number}}$	15	0.16	47.3	0.35	77.5 (++)
Δ_{AULRPC}	5-8-11-15 (kinetics)	0.12	67.2 (+)	0.50	86.7 (+++)
$\Delta_{\text{lateral_root_density}}$	5	0.06	66.5 (+)	0.75	68.8 (+)
$\Delta_{\text{lateral_root_density}}$	11	0.15	64.7 (+)	0.36	81.5 (++)
$\Delta_{\text{primary_root_length}}$	5	0.14	92.5 (+++)	0.22	56.6 (+)
$\Delta_{\text{primary_root_length}}$	11	0	82.1 (++)	0.36	69.9 (+)

798 +: $55 < \%_{\Delta > 0} < 70$, ++: $70 < \%_{\Delta > 0} < 85$, +++: $\%_{\Delta > 0} > 85$.

799

800

801

802
803
804
805
806
807
808
809
810
811
812
813
814
815

816 **Figure legends**

817 **Figure 1 –*Medicago truncatula* stimulation of root development by Fung- and Nod-LCOs**

818 Quantitative variation in the stimulation of root development is observed in response to (a)
819 Fung- and (b) Nod-LCOs, with 67% and 87% of the 173 accessions of *M. truncatula* showing
820 stimulation of root development, respectively. This root development was measured for 15
821 days and expressed as the delta_AULRPC (see Fig. S2). The position of the reference
822 genotype A17, relative to the other accessions, is indicated by a red arrow head. (c) Plot of
823 delta_AULRPC (Nod-LCOs – CTRL) values versus delta_AULRPC (Fung-LCOs – CTRL)
824 values and (d) plot of delta_LR_5d (Nod-LCOs – CTRL) versus delta_LR_5d (Fung-LCOs –
825 CTRL) values for 173 accessions of *Medicago truncatula*, indicating a weak correlation
826 between the stimulation by Fung- and Nod-LCOs. Vertical and horizontal dashed lines
827 indicate equal states of root development between treatment (Fung- or Nod-LCOs) and
828 control conditions (CTRL). The reference genotype A17 is indicated in red.

829

830 **Figure 2 – GWAS results using a local score approach on *Medicago truncatula***
831 **stimulation of lateral root development by Fung- and Nod-LCOs.**

832 Each Manhattan plot shows on the y-axis the Lindley process (the local score with the tuning
833 parameter $\xi = 3$) for SNPs along the eight chromosomes (x-axis), with the dashed line
834 indicating the maximum of the eight chromosome-wide significance thresholds. The local

835 score is shown for GWAS of four phenotypic variables: (a) delta_AULRPC (Fung-LCOs –
836 CTRL), (b) delta_AULRPC (Nod-LCOs – CTRL), (c) delta_LRD_5d (Fung-LCOs – CTRL)
837 and (d) delta_LRD_5d (Nod-LCOs – CTRL). The most significant candidate genes and their
838 predicted functions are indicated by arrows on the plots (see Table S1).

839

840 **Figure 3 – Gene ontology enrichment for the Nod-LCOs and Fung-LCOs candidate loci**
841 **identified by GWAS (local score results) in *Medicago truncatula***

842 Graphical summary of the gene ontology (GO) classification ranking of Fung-LCO candidate
843 genes (a, 71/105 represented) and Nod-LCO candidate genes (b, 134/183 represented) using
844 the Classification SuperViewer tool from bar.utoronto.ca adapted to *Medicago truncatula*.
845 Bars represent the normed frequency of each GO category for the given sets of genes
846 compared to the overall frequency calculated for the Mt4.0 *Medicago truncatula* (see
847 Herrbach *et al.*, 2017).

848 Hence, a ratio above 1 means enrichment and below 1 means under-representation. Error bars
849 are standard deviation of the normed frequency calculated by creating 100 gene sets from the
850 input set by random sampling and computing the frequency of classification for all of those
851 data sets across all categories. Hypergeometric enrichment tests on the frequencies were
852 performed and GO categories showing significant *p*-values (< 0.05) are printed bold. GO
853 categories are displayed for each GO subclass ranked by normed frequency values.

854

855

856

857

858

859

860

861

862

863

864

865

866

867

868

869

870

871

872

873

874

875

876

877

878

879

880

881

882

883

884 **Supplemental Figure legends**

885 **Figure S1. Structures of the LCOs used in this study compared to the “original” Myc-
886 LCOs as described in Maillet *et al.*, 2011.**

887 The Fung-LCO molecules used in this study belong to the class of LCOs most commonly
888 found in fungi (Rush *et al.*, 2020): LCO-V(C18:1, Fucosylated/MeFucosylated). The Nod-
889 LCOs used are specific to *S. meliloti*, rhizobial partner of *M. truncatula* (Roche *et al.*, 1991b),
890 mainly comprising LCO-IV(C16:2, Ac, S). As lipo-chitooligosaccharides, Fung-LCOs and
891 Nod-LCOs have the same canonical structure but also differences such as their number of
892 chitin residues (5 for Fung-LCOs and 4 for Nod-LCOs), their acyl chain on the non-reducing
893 end (C18:1 for Fung-LCOs and C16:2 for Nod-LCOs) and their substituents on the reducing
894 end (fucosyl or methylfucosyl for Fung-LCOs and sulfate for Nod-LCOs). The structures of
895 the original Myc-LCOs described by Maillet *et al.*: LCO-IV(C16:0, S or C18:1, S) or LCO-
896 IV(C16:0 or C18:1) (Maillet *et al.*, 2011) are also shown for comparison.

897

898 **Figure S2. Lateral root formation phenotypic variables used in this study.**

899 Stimulation of *Medicago truncatula* root development with Fung- or Nod LCOs was
900 monitored at different time-points (5, 8, 11 and 15 days post treatment), by counting lateral

901 root number (LR), measuring primary root length (RL), calculating lateral root density (LRD,
902 the ratio LR/RL) and measuring the Area Under the Lateral Root Progress Curve – AULRPC.

903

904

905

906

907

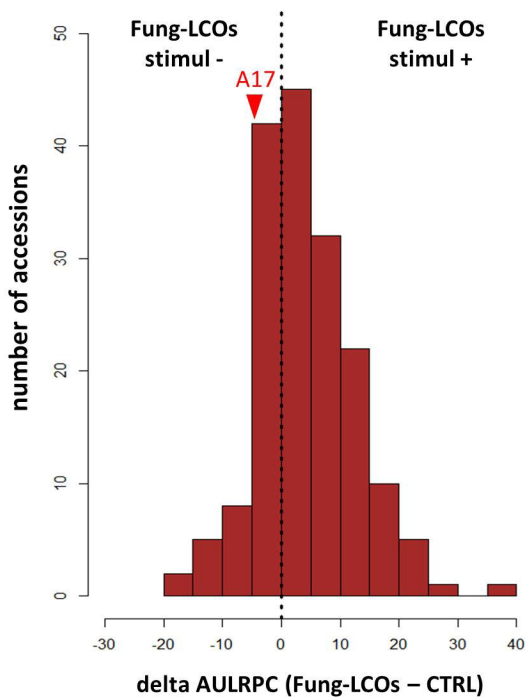
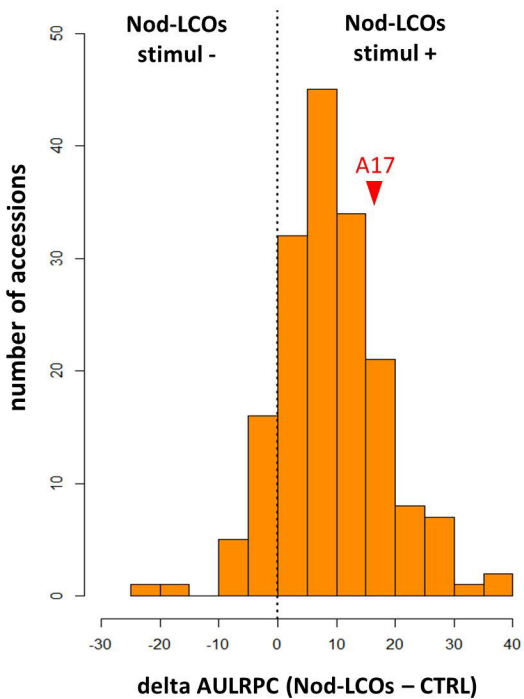
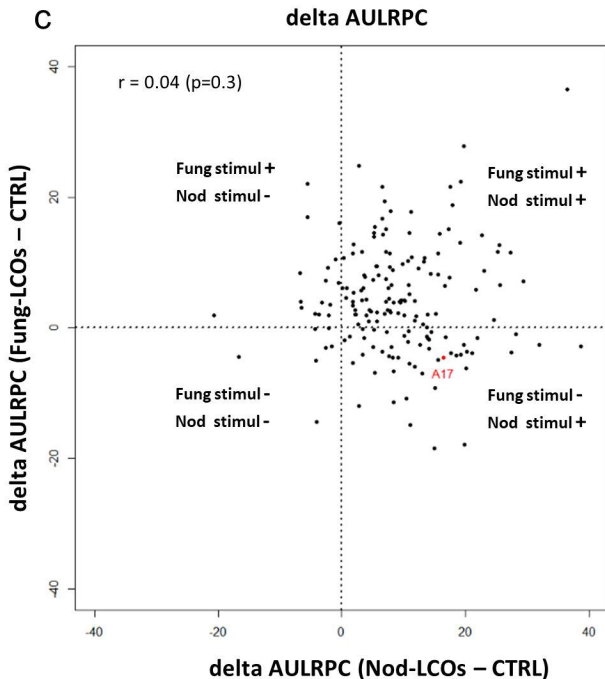
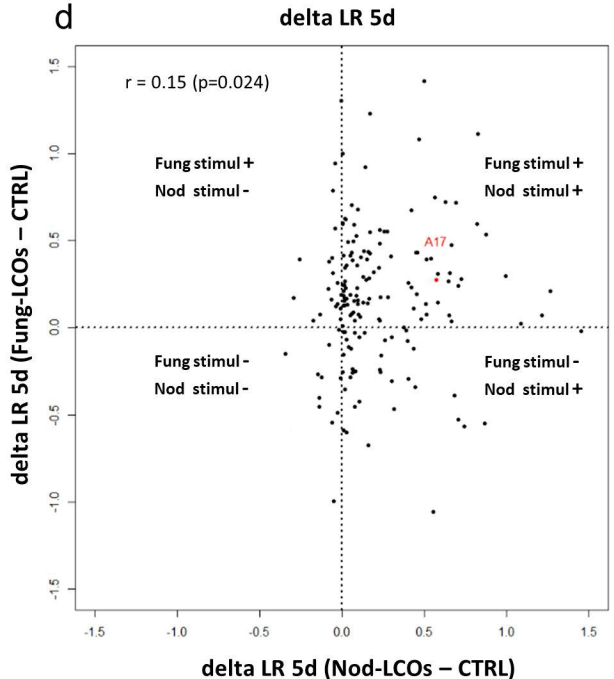
908

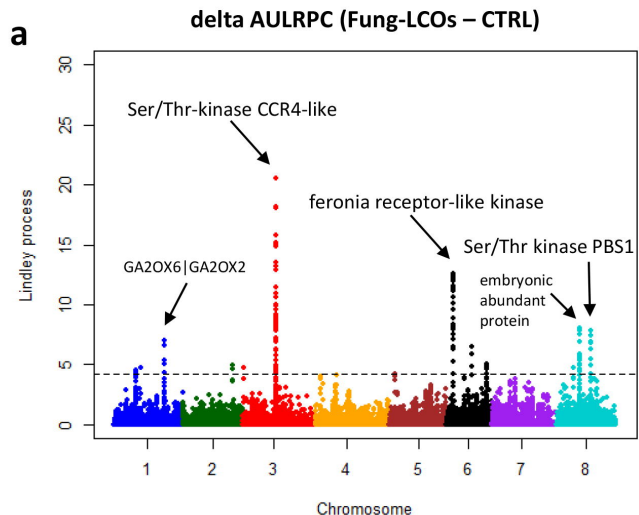
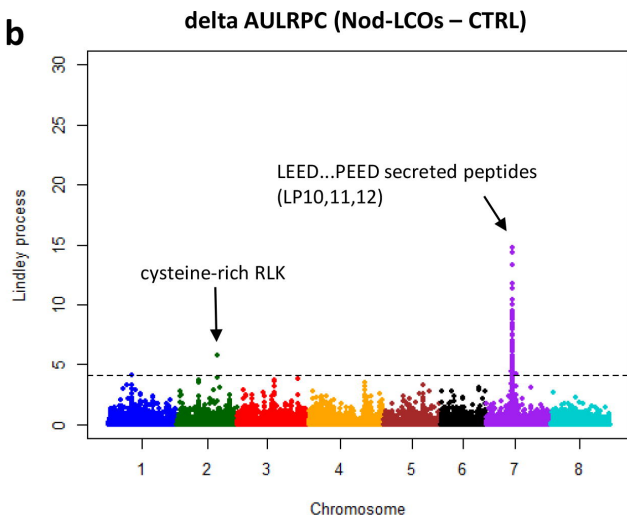
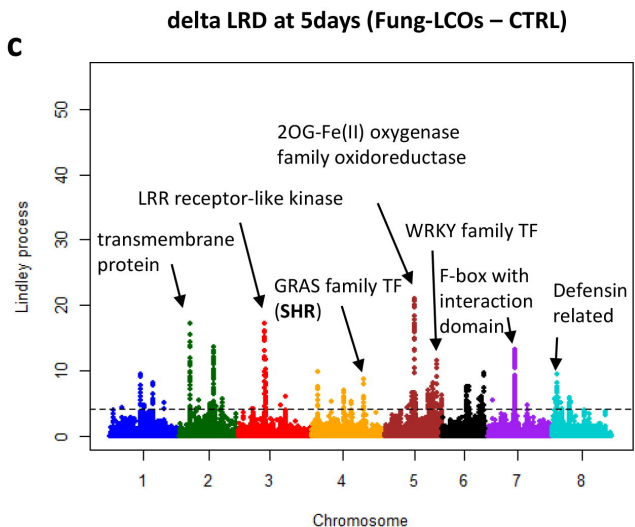
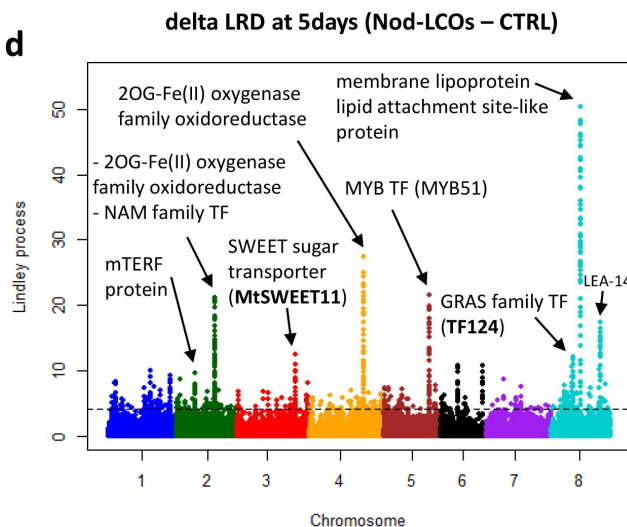
909

910

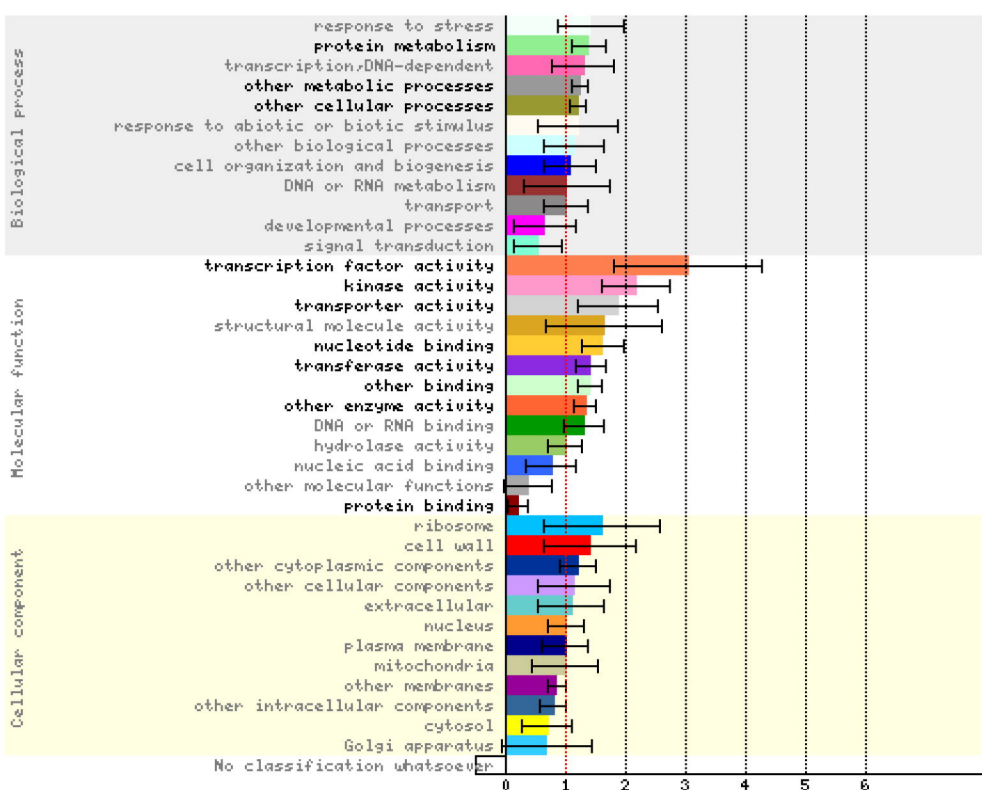
911

912

a**b****c****d**

a**b****c****d**

a. Fung-LCO genes (71/105 classified)



b. Nod-LCO genes (134/183 classified)

